PROCEEDINGS OF THE ROYAL SOCIETY A

Proc. R. Soc. A (2006) **462**, 3343–3362
doi:10.1098/rspa.2006.1720
Published online 25 May 2006

Adaptive importance sampling for risk analysis of complex infrastructure systems

By Richard Dawson* and Jim Hall

School of Civil Engineering and Geosciences, University of Newcastle upon Tyne, Cassie Building, Newcastle upon Tyne NE1 7RU, UK

Complex civil infrastructure systems are typically exposed to random loadings and have a large number of possible failure modes, which often exhibit spatially and temporally variable consequences. Monte Carlo (level III) reliability methods are attractive because of their flexibility and robustness, yet computational expense may be prohibitive, in which case variance reduction methods are required. In the importance sampling methodology presented here, the joint probability distribution of the loading variables is sampled according to the contribution that a given region in the joint space makes to risk, rather than according to probability of failure, which is the conventional importance sampling criterion in structural reliability analysis. Results from simulations are used to intermittently update the importance sampling density function based on the evaluations of the (initially unknown) risk function. The methodology is demonstrated on a propped cantilever beam system and then on a real coastal dike infrastructure system in the UK. The case study demonstrates that risk can be a complex function of loadings, the resistance and interactions of system components and the spatially variable damage associated with different modes of system failure. The methodology is applicable in general to Monte Carlo risk analysis of systems, but it is likely to be most beneficial where consequences of failure are a nonlinear function of load and where system simulation requires significant computational resources.

Keywords: importance sampling; infrastructure systems management; risk assessment; dike system; flood and coastal defence; structural reliability

1. Introduction

Risk, here defined as a function of probability and consequence, provides a rational basis for infrastructure system planning, design, operation and maintenance (Royal Society 1983, 1992; NRC 1992; Stewart & Melchers 1997; HM Treasury 2001). Engineering theory and, to some extent, practice dwells upon probability of failure as a measure of the performance of an infrastructure system, enabling engineers, in theory at least, to optimize the behaviour of the system to satisfy specified failure rate conditions. Reliability techniques (e.g. Thoft-Christensen & Baker 1982; Melchers 1999) focus upon accurately estimating the probability of system failure. Many safety critical systems are designed to a very low failure probability, usually because the consequences of

* Author for correspondence (richard.dawson@newcastle.ac.uk).

Received 1 November 2005
Accepted 20 March 2006

any type of failure are unacceptably catastrophic (e.g. loss of containment of a nuclear reactor), so in this case failure probability acts as an operational proxy for risk. This is a special case because often the failure state (the combination of one or more component failures that have caused system failure) and loading which results in system failure will determine the severity of the consequences (and perhaps their spatial heterogeneity). As will be demonstrated in this paper, the conditions resulting in the greatest probability of failure do not necessarily result in the greatest contribution to risk.

For a discrete system of moderate complexity, there are a combinatorially large number of possible system states. If, as is often the case, estimation of the probability of failure and consequences of any given system state involves computationally expensive simulation, the resources required to analyse all possible states may be infeasible. Our objective here is, however, different, aimed at estimating risk. *A priori* we do not know where the maximum risk is located in the space of the basic variables of the system and so we propose an adaptive method for progressively refining the risk estimate.

Following this introductory section, the relevant principles of risk analysis for infrastructure systems are introduced. Aspects of reliability theory and importance sampling are reviewed. Next, the adaptive risk-based importance sampling methodology is introduced. Two example applications are described, beginning with a propped cantilever beam to demonstrate the adaptive nature of the sampling and verify the approach for a simple system with an analytical solution. The methodology is then applied to a substantial practical case of a coastal dike system at Towyn in the UK, before concluding with discussion of the benefits and limitations of the proposed approach.

2. Reliability and risk analysis of systems

Consider a system consisting of t basic variables $\boldsymbol{x} := (x_1, \ldots, x_t)$ in $\mathcal{X}$, where $\mathcal{X} \subseteq \mathbb{R}^t$. The limit state function $g(\boldsymbol{x})$ separates the 'failed' region $\mathcal{G} = \{\boldsymbol{x} : g(\boldsymbol{x}) \leq 0\}$ from the 'not failed' region $\mathcal{G}' = \{\boldsymbol{x} : g(\boldsymbol{x}) > 0\} : \mathcal{G} \cup \mathcal{G}' = \mathcal{X}$. The probability of failure, p_f, is therefore the probability that the limit state function is less than or equal to zero:

$$p_\mathrm{f} = p(g(\boldsymbol{x}) \leq 0) = \int_{\mathcal{X}} I(g(\boldsymbol{x}) \leq 0)\rho(\boldsymbol{x})\mathrm{d}\boldsymbol{x}, \tag{2.1}$$

where $I(\cdot)$ is the indicator function and $\rho(\boldsymbol{x})$ is the joint probability density function (j.p.d.f.) of $\boldsymbol{x}$ on $\mathcal{X}$.

Methods of reliability analysis are customarily presented at three levels (JCSS 1981). Level I methods, in which partial safety factors are imposed on the loading and resistance variables, are now widely employed in limit state design codes. For level II methods, the failure surface is approximated with a first- or higher-order Taylor series expansion around the failure point closest to the origin (the 'design point') after the j.p.d.f. of the basic variables has been transformed into independent standardized normally distributed variables. Level II methods are efficient and elegant, but the approximation of the failure surface can be inaccurate for highly nonlinear limit state functions and relies upon an explicit limit state function, which may not be available. In level III methods, the integral

of the j.p.d.f. for the basic variables (2.1) is solved numerically. These are more flexible than level II methods, as both implicit and explicit limit state functions can be employed. However, level III methods can be computationally demanding.

If it is assumed that damage, c, occurs when the system is in a 'failed' state, then the risk, r, associated with the system is

$$r = \int_{\mathcal{X}} I(g(\boldsymbol{x}) \leq 0)\rho(\boldsymbol{x})c \, \mathrm{d}\boldsymbol{x}, \tag{2.2}$$

where c may be expressed in terms of economic damage or some other quantified measurement of harm. In general, however, the amount of damage will depend upon the values of $\boldsymbol{x}$ when failure takes place, which also determines the modes of failure in systems with multiple failure modes. We therefore replace c with a function $c(\boldsymbol{x})$:

$$c(\boldsymbol{x}) = \begin{cases} c(\boldsymbol{x}) = 0 & : \quad g(\boldsymbol{x}) > 0, \\ c(\boldsymbol{x}) > 0 & : \quad g(\boldsymbol{x}) \leq 0. \end{cases} \tag{2.3}$$

The risk calculation is therefore

$$r = \int_{\mathcal{X}} \rho(\boldsymbol{x})c(\boldsymbol{x})\mathrm{d}\boldsymbol{x}. \tag{2.4}$$

The existence of a limit state function may be thought of as being implicit in equation (2.4).

Like the reliability problem (2.1), transformation techniques may be applied to yield analytical solutions to equation (2.4), while numerical approximation methods are more flexible. However, for many systems, the function $c(\boldsymbol{x})$ may be implicit and, for each point $\boldsymbol{x}$, computationally expensive to estimate.

3. Integral estimation and variance reduction

Direct sampling, or 'Monte Carlo' analysis can be used to estimate the integral, ξ, of a function $f(\boldsymbol{x})$ over $\mathcal{T} \subset \mathcal{X}$:

$$\xi = \int_{\mathcal{X}} I_{\mathcal{T}}(\boldsymbol{x})f(\boldsymbol{x})\mathrm{d}\boldsymbol{x}. \tag{3.1}$$

If $\mathcal{T}$ is transformed to a unit hypercube, then, given n random input vectors, $\{\boldsymbol{x}_1, \ldots, \boldsymbol{x}_n\}$, uniformly distributed over $[0,1]^t$, the estimator $\hat{\xi}$ of ξ is

$$\hat{\xi} = \frac{1}{n}\sum_{j=1}^{n} f(\boldsymbol{x}_j). \tag{3.2}$$

The sample variance is given by

$$\mathrm{var}(\hat{\xi}) = \frac{1}{n-1}\left(\sum_{j=1}^{n} f(\boldsymbol{x}_j)^2 - \frac{1}{n}\left(\sum_{j=1}^{n} f(\boldsymbol{x}_j)\right)^2\right). \tag{3.3}$$

The variance reduces as n increases. A number of variance reduction techniques can be employed to increase the efficiency of the convergence (Morgan 1984; Ripley 1987; Melchers 1999), e.g. antithetic variables, stratified sampling and directional sampling. The goal of importance sampling, another variance reduction technique, is to reweigh the distribution of the random samples used in the Monte Carlo estimate, so that more samples are located in

regions where the integrand is larger. Equation (3.1) is rewritten as

$$\xi = \int_{\mathcal{X}} I_{\mathcal{T}}(\boldsymbol{x}) \frac{f(\boldsymbol{x})}{h(\boldsymbol{x})} h(\boldsymbol{x}) \mathrm{d}\boldsymbol{x}, \quad h(\boldsymbol{x}) > 0 \ \ \forall\, \boldsymbol{x} : f(\boldsymbol{x}) \neq 0, \tag{3.4}$$

where $h(\boldsymbol{x})$ is an importance sampling function and $\int_{\mathcal{X}} h(\boldsymbol{x})\mathrm{d}\boldsymbol{x} = 1$. More efficient sampling is achieved when $h(\boldsymbol{x})$ resembles the shape of the region of interest. A more efficient estimator compared to equation (3.2) is therefore

$$\hat{\xi} = \frac{1}{n} \sum_{j=1}^{n} \frac{f(\boldsymbol{x}_j)}{h(\boldsymbol{x}_j)}, \tag{3.5}$$

where $\boldsymbol{x}_1, \ldots, \boldsymbol{x}_n$ are random input vectors sampled from $h(\boldsymbol{x})$. The variance of the importance sampling estimator is

$$\mathrm{var}(\hat{\xi}) = \frac{1}{n} \sum_{j=1}^{n} \frac{f^2(\boldsymbol{x}_j)}{h(\boldsymbol{x}_j)} - \hat{\xi}^2. \tag{3.6}$$

In the context of the reliability problem (2.1), the importance sampling estimator is

$$\hat{p}_{\mathrm{f}} = \frac{1}{n} \sum_{j=1}^{n} I(g(\boldsymbol{x}) \leq 0) \frac{\rho(\boldsymbol{x}_j)}{h(\boldsymbol{x}_j)}. \tag{3.7}$$

In this case, the importance sampling function, $h(\boldsymbol{x})$, is most efficient when it is proportional to $I(g(\boldsymbol{x} \leq 0))\rho(\boldsymbol{x})$.

4. Adaptive risk-based sampling methodology

The damage function $c(\boldsymbol{x})$, introduced earlier, is seldom straightforward and may require expensive numerical solution, making it difficult to presuppose which states of the basic variables contribute most to the risk, r. We therefore address the situation where it is infeasible to do a very large number of evaluations of the function $c(\boldsymbol{x})$.

Algorithms of an adaptive nature have been demonstrated on reliability problems by Bucher (1988) and Melchers (1990). Their method uses sample outcomes to update the location of the mean of the importance sampling function, $h(\boldsymbol{x})$, such that the mean is gradually relocated nearer the location of the maximum likelihood. While $h(\boldsymbol{x})$ could be multi-modal, the form of the function is not updated during the analysis, and so a successful outcome is still dependent on selecting an initial appropriate form for $h(\boldsymbol{x})$.

In this section, we propose a method that makes use of a non-parametric importance sampling function that seeks to approximate $\rho(\boldsymbol{x})c(\boldsymbol{x})$. We achieve this in the first instance with an exploratory analysis of the function $r^*(\boldsymbol{x}) = \rho(\boldsymbol{x})c(\boldsymbol{x})$ and progressively refine the estimate of risk (the numerical estimate of the integral in equation (2.4)) by means of a non-parametric adaptive risk-based importance sampling function, written as $h_{r,n}(\boldsymbol{x})$, where n signifies the cumulative number of samples in the adaptive process.

Little is known about $r^*(\boldsymbol{x})$ at the outset of an analysis, so the initial exploration of $r^*(\boldsymbol{x})$ necessarily spans the whole of the region $\mathcal{A} \subseteq \mathcal{X}$, where $r^*(\boldsymbol{x})$ is known to be non-negligible. In the absence of further information, the exploratory sample is uniform throughout $\mathcal{A}$. This could be achieved by selecting samples on a regular grid over $\mathcal{A}$, or by randomly sampling from a multi-variate

uniform distribution over $\mathcal{A}: h_{r,n_0}(\boldsymbol{x}) \sim U(\mathcal{A})$. Starting with a random sample from a known distribution is attractive, because the n_0 initial samples can subsequently contribute to the pool of random samples used in the integral estimation without biasing the pool. We would like this initial sample to be reasonably evenly spread over $\mathcal{A}$, so in practice we try a large number of sets of n_0 random samples from $h_{r,n_0}(\boldsymbol{x})$ and select the set of samples that minimizes b_0:

$$b_0 = \sum_{i=1}^{t} \sum_{j=1}^{n_0-1} \left(\frac{l_i}{n_0 - 1} - d_{i,j} \right)^2, \tag{4.1}$$

where l_i is the length of the projection of $\mathcal{A}$ onto the x_i-axis and $d_{i,j}$ is the distance on the x_i-axis between points x_j and x_{j+1}. By doing so, we ensure that the samples from $U(\mathcal{A})$ are reasonably evenly spread over A and extend towards the boundaries of the region.

The risk is evaluated at each of the n samples. A function based on these n evaluations of risk, $h_{r,n}(\boldsymbol{x})$, is obtained by fitting a surface over the n evaluations of risk $r^*(\boldsymbol{x}_j) : j = 1, \ldots, n$. This risk function is normalized to give the j.p.d.f. $h_{r,n}(\boldsymbol{x})$, henceforth referred to as the risk-based importance sampling function. The next set of points, $\{\boldsymbol{x}_j : j = n+1, \ldots, n'\}$ at which $r^*(\boldsymbol{x}_j)$ is evaluated, are subsequently sampled from $h_{r,n}(\boldsymbol{x})$.

As more samples of $\boldsymbol{x}_j$ and estimates of $r^*(\boldsymbol{x}_j)$ are obtained, the importance sampling function $h_{r,n}(\boldsymbol{x})$ can be intermittently updated. The updating should be frequent enough so that the sampling routine benefits from the improved sampling function, but not so frequent that the process of updating becomes a computational burden in its own right, which may be significant for higher-dimensional problems. The update frequencies used in the following case studies are within the range of 20–100 proposed for alternative adaptive methods (Melchers 1990). The estimator $\hat{r}_n$ of total risk after n samples is

$$\hat{r}_n = \frac{1}{n} \sum_{j=1}^{n} \frac{r^*(\boldsymbol{x}_j)}{h_{r,j}(\boldsymbol{x}_j)}, \tag{4.2}$$

where $h_{r,j}$ is the risk-based importance sampling distribution from which sample $\boldsymbol{x}_j$ is chosen. For samples $j = 1, \ldots, n_0$, the (non-risk-based) uniform sampling function, $h_{r,n_0}(\boldsymbol{x})$, is employed. The process of estimating the total risk, $\hat{r}_n$, and updating the sampling distribution is repeated until the specified convergence criterion is satisfied.

Except in the special case of $c(\boldsymbol{x})$ being a positive constant over $\mathcal{G}$ and zero elsewhere in $\mathcal{X}$, it is clear that the importance sampling function used in the reliability problem, $h(\boldsymbol{x})$, and the risk-based importance sampling function, $h_{r,n}(\boldsymbol{x})$, will not be the same. In many cases, $h(\boldsymbol{x})$ will be a poor sampling function for estimating r.

This same adaptive approach could also be used in the reliability problem to estimate the probability of failure $\hat{p}_{\mathrm{f},n}$ after n samples, where the importance sampling function, $h(\boldsymbol{x})$, is updated intermittently by fitting a surface to $I(g(\boldsymbol{x}) \leq 0)\rho(\boldsymbol{x}_j)$:

$$\hat{p}_{\mathrm{f},n} = \frac{1}{n} \sum_{j=1}^{n} I(g(\boldsymbol{x}) \leq 0) \frac{\rho(\boldsymbol{x}_j)}{h_j(\boldsymbol{x}_j)}, \tag{4.3}$$

where $h_j(\boldsymbol{x}_j)$ is the importance sampling function from which $\boldsymbol{x}_j$ is chosen.

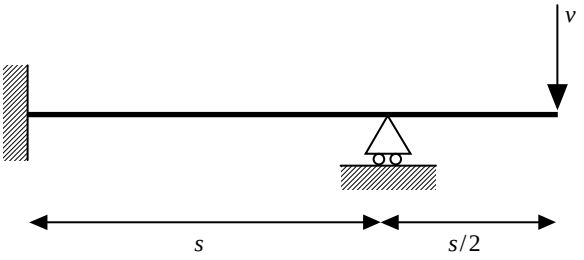

Figure 1. Propped cantilevered beam with vertical load imposed.

5. A simple system: propped cantilever beam

The adaptive risk-based importance sampling methodology is demonstrated by considering a simple reliability problem, that of a beam of length $1.5s$ with a concentrated vertical random load, V, imposed on its cantilever end (figure 1). For this system, damage occurs only when $|M| \geq M_c$, where $|M|$ is the maximum bending moment in the beam and M_c is the (random) critical moment capacity. Hence, if $s=5$ m the limit state function, $g(Z)$, is

$$g(Z) = M_c - \frac{sV}{2} = M_c - \frac{5}{2}V. \tag{5.1}$$

The basic variables V and M_c are assumed to be uncorrelated, normally distributed variables: $V \sim N(25, 5)$ kN and $M_c \sim N(100, 10)$ kN m.

The fragility, $p(Z \leq 0 | V = v)$, of the beam and the loading probability, $\phi(v)$, are plotted in figure 2. The system probability of failure is 9.57×10^{-3}. In this case, damage occurs only when $m_c - (5/2) \leq 0$ and increases with load:

$$\left.\begin{aligned} c(v) &= 3^v : m_c - \frac{5}{2}v \leq 0, \\ c(v) &= 0 : m_c - \frac{5}{2}v > 0. \end{aligned}\right\} \tag{5.2}$$

The risk function for this problem is therefore

$$r = \int_0^\infty \int_0^\infty \rho(v, m_c) c(v) \mathrm{d}v \, \mathrm{d}m_c. \tag{5.3}$$

Figure 2 plots $c(v)$ against v, given that $m_c - (5/2)v \leq 0$. The analytical solution to equation (5.3) gives a total risk, $\hat{r} = £2.94 \times 10^{18}$.

Four sampling strategies were tested (figure 3).

(i) *Uniform Monte Carlo approach.* Each sample $\boldsymbol{x}_j := (v_j, m_{cj}) : j = 1, \ldots, n$ is sampled from $v_j \sim U(0, 100)$ and $m_{cj} \sim U(0, 200)$. These distributions were selected to ensure coverage of the whole area, for which the probability and the consequences of failure are non-negligible.

(ii) *Crude Monte Carlo approach.* Realizations of $\boldsymbol{x}_j$ were sampled randomly from the distributions of the basic variables V and M_c.

(iii) *Adaptive probabilistic importance sampling.* The importance sampling distribution $h(\boldsymbol{x})$, as defined in equation (3.7) (i.e. based on the probability of structural failure), was used. The starting values

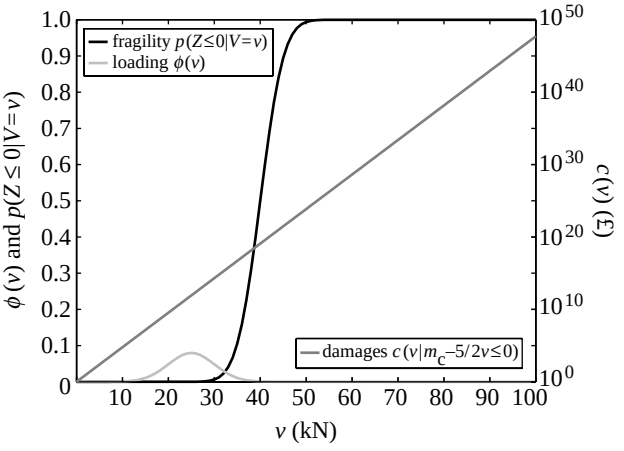

Figure 2. The loading distribution (left axis), fragility (left axis) and damage (right axis, log scale) associated with the beam in figure 1.

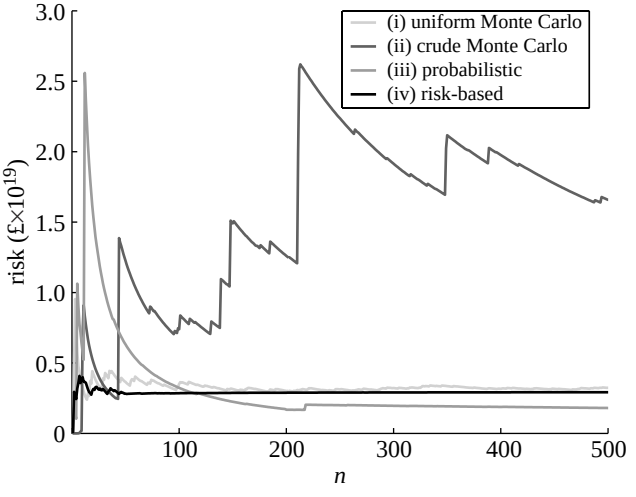

Figure 3. Comparing the convergence of the four sampling strategies.

and update frequencies were as used in the adaptive risk-based sampling strategy. In this case, after 200 simulations, the projection $h_n(v)$ corresponds well with the analytically derived version of $I(g(v)\leq 0)\phi(v)$.

(iv) *Adaptive risk-based importance sampling.* The initial exploratory analysis for the risk-based sampling strategy was simulated at $v=\{0.3, 21.02, 40.16, 58.38, 77.10, 96.94\}$ kN and $m_c=\{0.15, 40.01, 79.83, 119.78, 160.03, 199.22\}$ kN m. These points were chosen from 10^6 sets of six samples of $h_{r,n_0}(\boldsymbol{x})$ and minimized the quantity b_0 (4.1) at $b_0=19.26$. Subsequently, $h_{r,n}(\boldsymbol{x})$ was updated every 25 realizations. Intermittent plots of the sampling distribution, showing only the projection on v for clarity, are shown in figure 4. As with the adaptive probabilistic sampling strategy, after 200 simulations, the projection $h_{r,n}(v)$ corresponds well with the analytically derived version of $r^*(v)$.

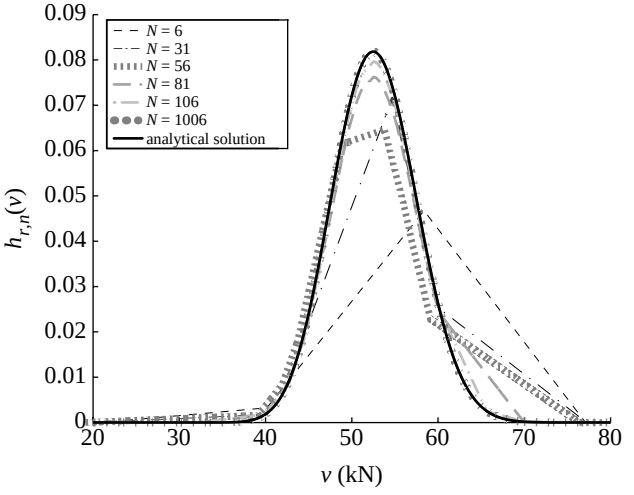

Figure 4. Iterations of the risk-based importance sampling distribution (projected onto v) starting at $N=6$ (i.e. after exploratory analysis) up to $N=1006$, which is barely separable from the analytical solution.

An empirical convergence criterion limiting the variation between the minimum and maximum estimate of the last 10% of samples to less than 0.1% of the estimate after n samples (tested when n is divisible by 10) was adopted:

$$\max(\hat{r}_{0.9n},\ldots,\hat{r}_n)-\min(\hat{r}_{0.9n},\ldots,\hat{r}_n)<0.001\left[\frac{1}{0.1n}\sum_{j=0.9n}^{n}\hat{r}_j\right]. \tag{5.4}$$

Using this criterion, sampling strategy (i) requires approximately 10^4 simulations, whereas using the risk-based sampling approach, strategy (iv), needs only 500 simulations to converge upon $\hat{r}=£2.94\times10^{18}$. Both these compare favourably with strategies (ii) and (iii), which do not meet the convergence criterion even after 10^6 realizations. In both these cases, the sampling is sparse in the region of maximum risk at $v=52.5$ kN.

Conventionally, the structural design point refers to point in the violation space of the limit state function with the greatest probability density. We therefore name the point that maximizes $r^*(\boldsymbol{x})$ as the risk-based design point of the system. In the case of the probability-based sampling strategy, (iii), the maximum sampling density is centred on the structural design point of the beam at $v=35.4$ kN. In this situation, the probability density at the risk-based design point is typically of the order 10^{-5}, therefore this strategy biases the sampling away from the region of interest making it difficult for the risk to converge, thus demonstrating the importance of selecting an appropriate sampling distribution (e.g. Schreider 1966; Melchers 1989; McKay 2003). Strategy (ii) is also less efficient than strategy (iv), but perhaps less intuitively it appears to be less efficient than strategy (i). This is because, in this particular example, the sampling density is actually greater in the region of interest under strategy (i) than strategy (ii).

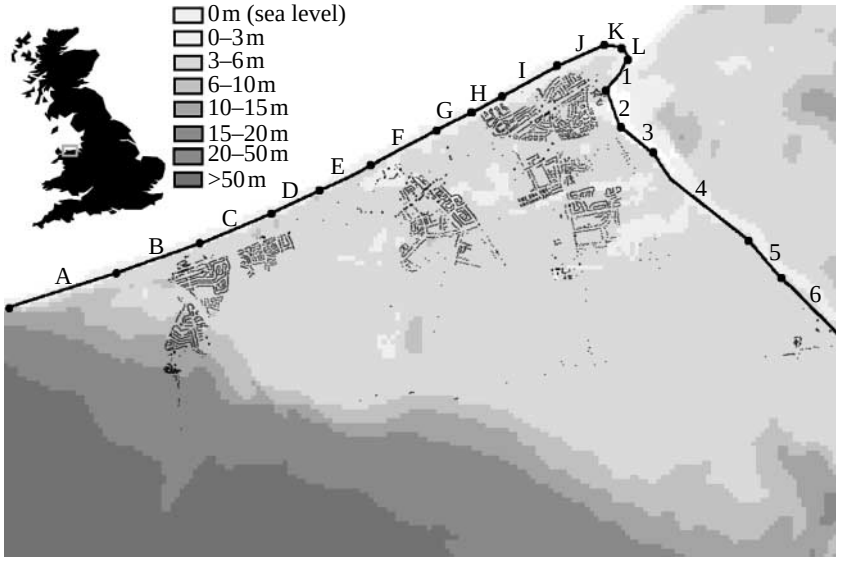

Figure 5. A map of Towyn (darker shades represent higher ground) showing the location of residential (lighter points) and non-residential (darker points) property and the dike sections (labelled A–K and 1–6).

6. A real system: coastal dike system

In England and Wales, 1 million properties worth over £130 billion and 430 000 hectares of agricultural land worth approximately £2 billion (Halcrow *et al.* 2001) are protected by some 1300 km of sea dike (Madrell *et al.* 1998). The case study site is Towyn in North Wales (figure 5). The town is built on large areas of coastal lowland that were reclaimed during the eighteenth century and was inundated in 1990 when 467 m of seawall was breached. Typically, a coastal dike system is characterized by

— two (partially correlated) loading variables, wave height, H_s, and water level, W,
— a system of q coastal dike components that may be overtopped by high waves and/or water levels and may fail structurally by breaching, and
— spatially variable location and type of assets susceptible to damage in the event of a flood.

In order to obtain realistic damage estimates in the event of wave overtopping or breaching failure, computationally demanding inundation modelling is necessary. An efficient sampling strategy is therefore required.

The five main requirements for calculating coastal flood risk are

(i) statistical estimation of extreme loads;
(ii) calculation of system reliability;
(iii) estimation of dike breach characteristics;

(iv) model inundation depth and extent due to wave overtopping or breaching of the dikes; and
(v) estimation of damage to individual properties resulting from inundation to a given depth.

An overview of the methodology as applied to the coastal dike system is shown in figure 6.

(*a*) *Statistical estimation of extreme loads*

A j.p.d.f. $\phi(H_s, W)$ for the (non-negative) loading variables $\boldsymbol{v} := (H_s, W)$ was constructed from simultaneous measurements of wave height, H_s, and water level, W, using the approach of Hawkes *et al.* (2002).

(*b*) *Systems reliability analysis*

The dike system in the example implementation comprises 12 coastal sections (labelled A–L) and six fluvial sections (labelled 1–6), of which four are raised ground and not prone to failure (figure 5).

For a system of q dike sections, labelled $d_1, \ldots, d_q$, the breaching of section d_i is labelled as D_i and non-breaching as $\neg D_i$. There are therefore 2^q possible system states, labelled $s_m : m = 1, \ldots, 2^q$, of which $2^q - 1$ refer to states with at least one breached component. The set of states in which one or more components has breached is labelled $\mathcal{S}$. Flooding may occur by water overtopping the dike even if the dike has not breached, but the consequences tend to be greater in the event of a breach. The consequence of failure is therefore a function, $c(s_m, \boldsymbol{v})$, of both the system state s_m and the load $\boldsymbol{v}$.

The probability of each of these states occurring will vary according to the (not necessarily independent) load, $\boldsymbol{v}$, imposed upon the system. Structural performance is described using a fragility function that describes the probability of breaching, conditional on a specific loading (Casciati & Faravelli 1991; Dawson & Hall 2003). The fragility function of system component i, given load $\boldsymbol{v}$, is therefore the conditional probability $p(D_i|\boldsymbol{v})$. The probability, $p(D_i)$, of breaching of a given component, D_i, can be established by integrating over the j.p.d.f. of loading, $\phi(\boldsymbol{v})$:

$$p(D_i) = \int_0^\infty p(D_i|\boldsymbol{v})\phi(\boldsymbol{v})\mathrm{d}\boldsymbol{v}. \tag{6.1}$$

The breaching failure modes considered are summarized in table 1 and four representative fragility functions are plotted over $H_s \times W$ in figure 7.

The main source of dependency between the components in this series systems originates from the loading, while the resistance of each section tends to be independent. The resistance of some dike sections, particularly those located near each other and sharing similar failure modes, may not be completely independent—perhaps due to shared geotechnical conditions. However, by using an appropriate length of dike sections, the resistance variables may be assumed to be independent (Van Gelder & Vrijling 1998), conditional upon loading. Sufficiently dense spatial testing of the strength parameters in the dikes would enable the correlation length to be estimated and expressions (5.4) and (6.1) modified accordingly (CUR and TAW 1990). However, assuming

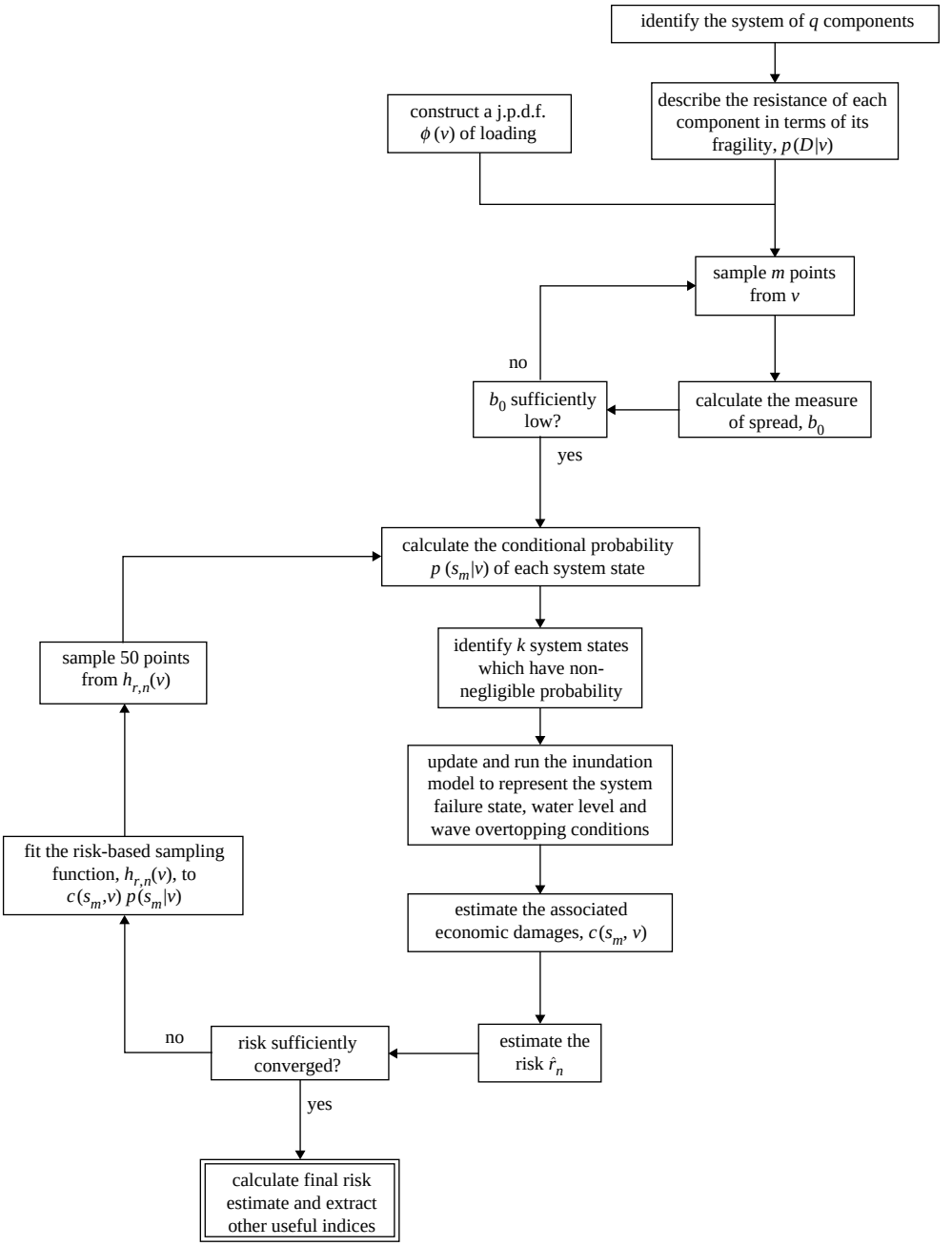

Figure 6. Overview of risk assessment methodology for coastal dike systems.

independence, conditional upon loading, the conditional probability of breaching failure of one or more components in series is

$$p(\mathcal{S}|\boldsymbol{v}) = 1 - \prod_{i=1}^{q} [1 - p(D_i|\boldsymbol{v})] \,. \tag{6.2}$$

Table 1. Summary of breaching failure modes used to generate dike fragility functions.

failure mode	description	equation(s) and variable definition (applies only to the associated equation in this table)		reference(s)
shingle beach erosion	shingle beach erosion leading to the collapse of a landward seawall	parametric resolution of beach shape after a storm event		Powell (1990, 1993)
overtopping	overtopping damage resulting in leeside damage or erosion of dike	$Q = A T_{\mathrm{m}} g H_{\mathrm{s}} \exp\left(-\left(B \frac{R_{\mathrm{c}}}{T_{\mathrm{m}}(gH_{\mathrm{s}})^{0.5}}\right)/r\right)$	A, B (empirical coefficients), r (roughness coefficient), T_{m} (mean wave period), H_{s} (significant wave height), R_{c} (freeboard)	HR Wallingford (1999)
rock armour damage	wave damage resulting in loss of rock armour revetment leading to dike failure	$H_{\mathrm{s}} = 6.2 S_{\mathrm{d}}^{0.2} P^{0.18} \Delta D_{\mathrm{n}}50(\cot\alpha)^{0.5} s_m^{0.25} N^{0.1}$ (plunging waves) $H_{\mathrm{s}} = S_{\mathrm{d}} P^{-0.13} \Delta D_{\mathrm{n50}} (\cot\alpha)^{(0.5-P)} s_m^{-0.5P} N^{-0.1}$ (surging waves)	S_{d} (the damage number), P (permeability factor), $\Delta = \rho_{\mathrm{rock}}/\rho_{\mathrm{water}} - 1$, ρ (density), D_{n50} (nominal rock diameter), α (revetment slope), s_m (mean wave steepness), N (number of waves)	Van der Meer (1988), CIRIA (1996)
dune erosion	erosion of dunes	parametric resolution of beach shape after a storm event		CUR & TAW (1990), CIRIA (1996)
piping	flow paths through embankments leading to breaching	$C_{\mathrm{w}} = \frac{B/3 \sum t}{H}$	C_{w} (the weighted creep ratio, based on embankment material), B (structure width), t (depth of impervious layers), H (head across embankment)	Terzaghi *et al.* (1996)

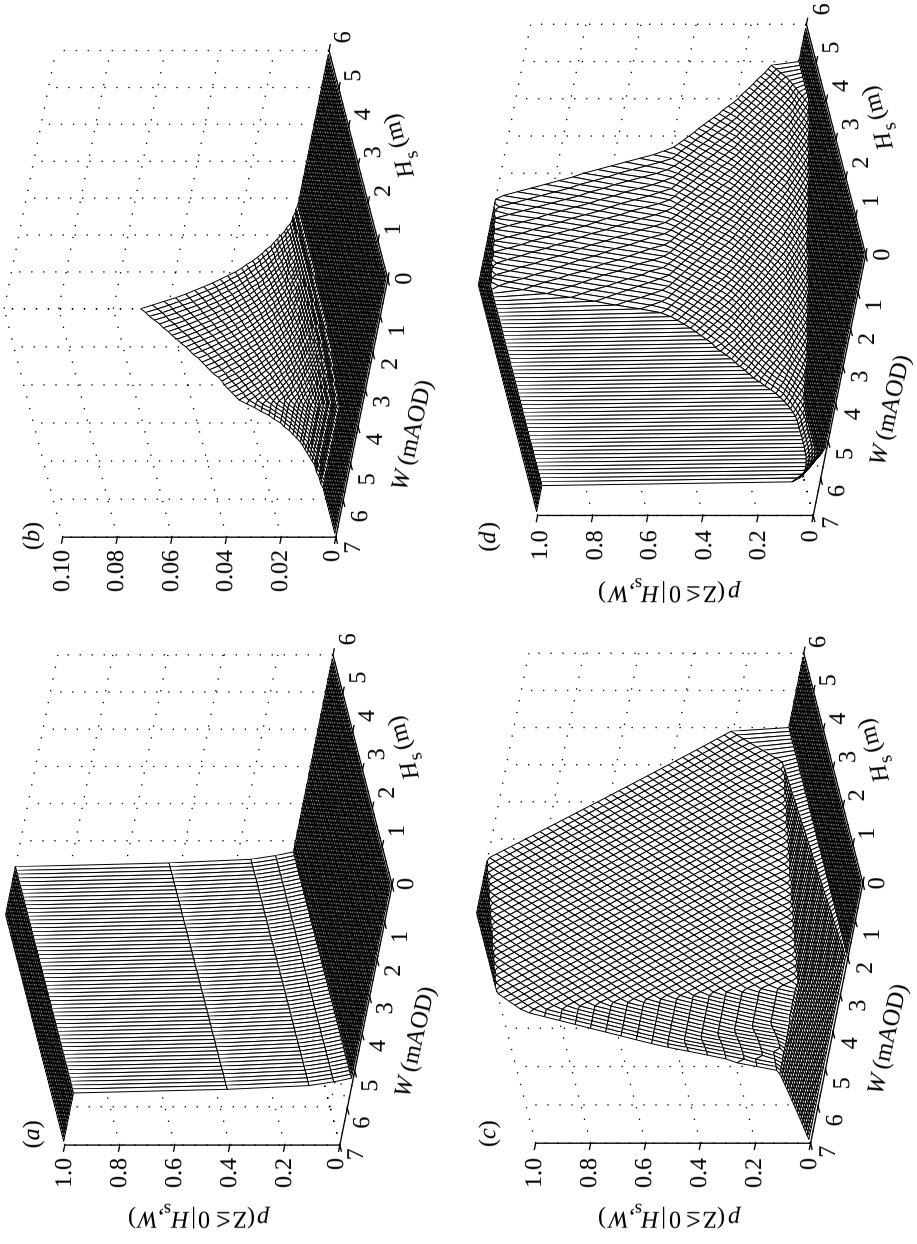

Figure 7. Dike fragility plotted over the loading space for four of the dikes. (*a*) Dike 4: piping failure. (*b*) Dike D: rock armour failure. (*c*) Dike K: dune erosion failure. (*d*) Dike I: shingle beach erosion failure. mAOD, metres Above Ordnance Datum.

The conditional probability of any given state s_m, for example corresponding to the event $D_1 \wedge \ldots \wedge D_m \wedge \neg D_{m+1} \wedge \ldots \wedge \neg D_q$, can be calculated as

$$p(s_m|\boldsymbol{v}) = \prod_{i=1}^{m} p(D_i|\boldsymbol{v}) \prod_{i=m+1}^{q} [1 - p(D_i|\boldsymbol{v})]. \tag{6.3}$$

The total flood risk is therefore

$$r = \int \sum_{m=1}^{2^q} p(s_m|\boldsymbol{v}) \phi(\boldsymbol{v}) c(s_m, \boldsymbol{v}) \mathrm{d}\boldsymbol{v}. \tag{6.4}$$

In order to reduce the number of system states analysed in evaluating $c(s_m, \boldsymbol{v})$, the k system states combinations that make a non-negligible contribution towards $\sum_{m=1}^{2^q} p(s_m|\boldsymbol{v}) = 1$ (generally $k \lll 2^q$) are selected. The definition of a non-negligible contribution depends on the required precision, and in this analysis a minimum requirement of $\sum_{m=1}^{k} p(s_m|\boldsymbol{v}) > 0.99$ was set. A lower bound on the total flood risk, expressed in terms of an expected annual economic damage for a coastal dike system, is therefore

$$\hat{r}_n^- = \frac{1}{n} \sum_{j=1}^{n} \sum_{m=1}^{k} \frac{p(s_m|\boldsymbol{v}_j) \phi(\boldsymbol{v}_j) c(s_m, \boldsymbol{v}_j)}{h_{r,j}(\boldsymbol{v}_j)}, \tag{6.5}$$

where by definition $\sum_{m=1}^{2^q} p(s_m|\boldsymbol{v}) = 1$ and $\int_0^\infty \phi(\boldsymbol{v}) \mathrm{d}\boldsymbol{v} = 1$.

An upper bound, $\hat{r}_n^+$, associated with not analysing every permutation of s_m can be estimated using

$$\hat{r}_n^+ = \hat{r}_n^- + \sum_{j=1}^{n} \left[\frac{\phi(\boldsymbol{v}_j) c_j^+}{h_{r,j}(\boldsymbol{v}_j)} \left(1 - \sum_{m=1}^{k} p(s_m|\boldsymbol{v}_j) \right) \right], \tag{6.6}$$

where c_j^+ is an estimate of the maximum possible damage for a given loading.

(c) *Dike breaching*

Prediction of dike breach location, geometry and growth rate is highly uncertain (Wahl 1998). A number of simplified rules for breach width have been proposed, including

$$B_\mathrm{w} = \min[10ha, B], \tag{6.7}$$

where B is the dike length, h is the overflow depth and a is as little as 3 for cohesive materials (HR Wallingford 2004) and as great as 15 for non-cohesive materials (Visser 1998). Here $a = 12$.

(d) *Inundation modelling*

Simulation of inundation over low-gradient floodplains with dike structures requires at least a two-dimensional hydrodynamic modelling approach with relatively high spatial resolution to represent the complex geometry of the floodplain. However, full two- or three-dimensional hydrodynamic modelling remains computationally prohibitive if multiple breach or overtopping cases are to be modelled. In order to reduce the computational burden of the hydrodynamic calculations for this study, a simplified two-dimensional inundation model called LISFLOOD-FP (Bates & De Roo 2000), which runs in a matter of seconds, was selected. This model generates a spatial field of water depths in the floodplain and has been shown to perform as well as full

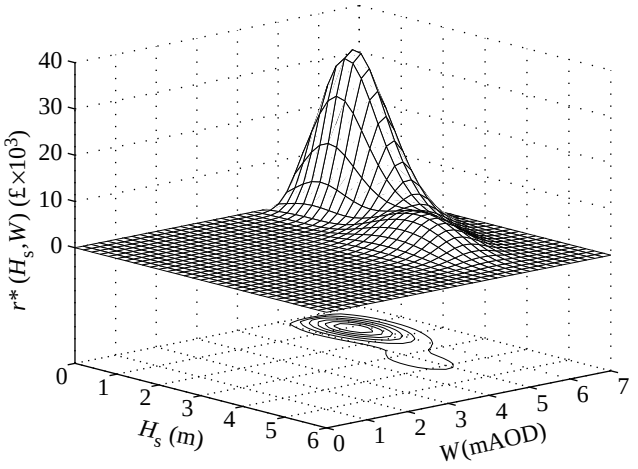

Figure 8. The function $r^*(\boldsymbol{v})$ plotted over $H_s \times W$.

two-dimensional codes (Horritt & Bates 2001). It has been successfully demonstrated at a number of coastal sites (Bates *et al.* 2005). The model was calibrated using data from the 1990 flood.

(*e*) *Damage estimation*

A national database combines information on property type and location in England and Wales. For each property type, Penning-Rowsell *et al.* (2003) have defined a depth–damage relationship.

(*f*) *Implementation of methodology*

An exploratory analysis of 49 loading points was simulated from $H_s \sim U(0,6)$, $W \sim U(1,7)$, with the quantity b_0 measured at $b_0 = 23.71$. Subsequently, $h_{r,n}(\boldsymbol{v})$ was updated every 50 realizations. The risk converged (according to the criterion defined in equation (5.4)) after testing 2000 realizations. The function describing the location of risk, $r^*(\boldsymbol{v})$, is shown in figure 8. The total risk, expressed in terms of expected annual damage, is approximately £84 000. The maximum risk occurs at $H_s = 1$ m, $W = 5.5$ m, with a secondary maxima at $H_s = 3.5$ m, $W = 4.5$ m. It is clear from inspection of $r^*(\boldsymbol{v})$ that a uniform sampling strategy over the loading space would result in over half of the samples contributing no information to the analysis.

The expected annual damages and expected annual inundation probability (defined as the probability of a water level, Y_W, greater than zero in a given grid cell) can be reported spatially. The map of inundation probability (figure 9, which also shows dike failure probabilities) shows that the majority of the floodplain has a 0.005–0.01 probability of flooding. This is dominated by the potential for piping failure of the estuary embankments. The West side of the floodplain is significantly less prone to flooding. Comparing this with the map of flood risk, figure 10 (which also shows contributions from each dike section to flood risk) demonstrates that there is not an exact correlation between risk and inundation probability.

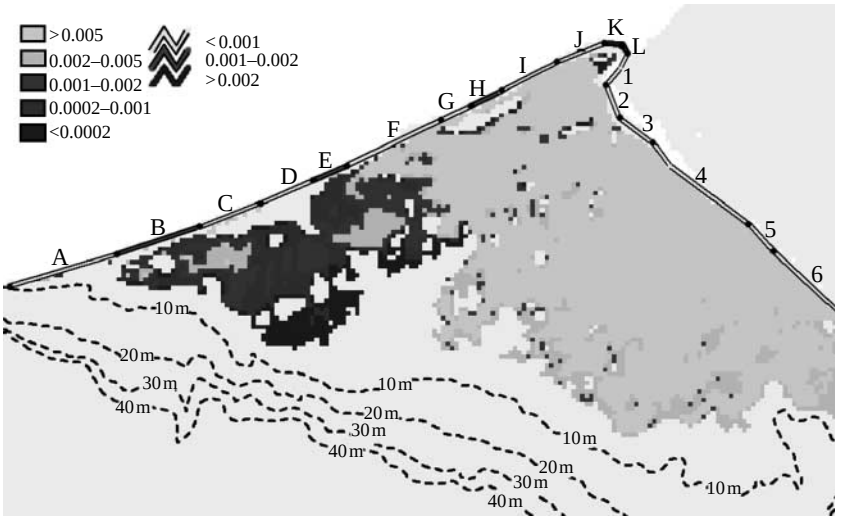

Figure 9. Spatial distribution of annual inundation probability, $p(Y_W > 0)$, and dike failure probability, $p(D_i)$. Floodplain relief not shaded, but indicated using contours at 10, 20, 30 and 40 m.

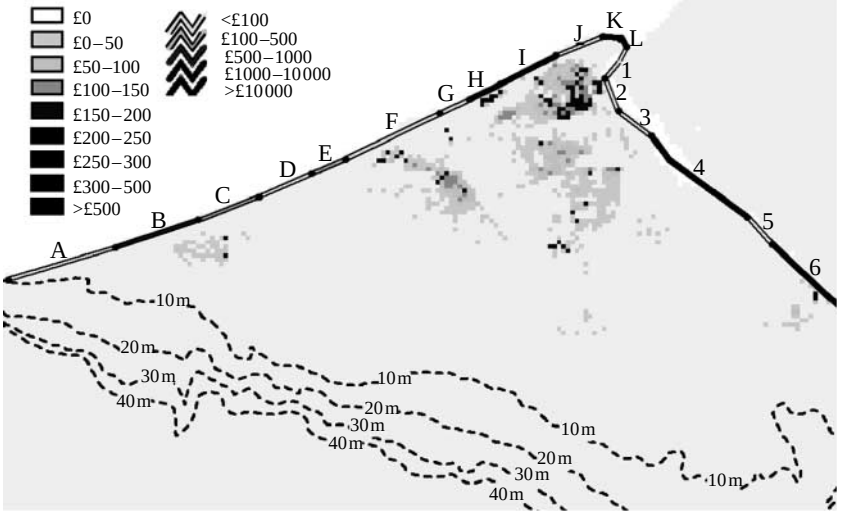

Figure 10. Spatial distribution of flood risk (in £s) with dike line shaded to represent contribution of dike towards flood risk (in £). Floodplain relief not shaded, but indicated using contours at 10, 20, 30 and 40 m.

(*g*) *Discussion*

Figure 11 compares the conditional systems failure probability, $p(\mathcal{S}|\boldsymbol{v})\phi(\boldsymbol{v})$, and $r^*(\boldsymbol{v})$. Three points corresponding to maxima are labelled; the largest,

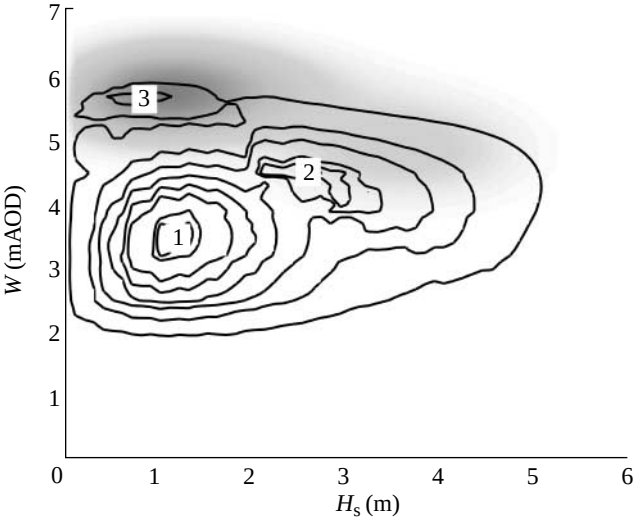

Figure 11. Comparison of $r^*(H_s, W)$ in shades of grey and $p(\mathcal{S}|H_s, W)$. $\phi(H_s, W)$ as contours over $H_s \times W$.

(1) $H_s = 1$ m, $W = 3.5$ m is dominated by $\phi(\boldsymbol{v})$, (2) $H_s = 2.75$ m, $W = 4.5$ m is dominated by failure mechanisms influenced by joint loading conditions (e.g. beach erosion and revetment damage), (3) $H_s = 0.8$ m, $W = 2$ m is dominated by the piping failure of the estuarial dikes (which is influenced by W alone). The system design point does not therefore correspond with the maximum risk, because the topography is such that only a storm surge greater than approximately 4 metres Above Ordnance Datum (mAOD) results in any significant inundation, while a surge of approximately 5 mAOD is required for $c(\boldsymbol{v}) > £1$ million. Overtopping events at lower water levels do occur, but do not release sufficient water into the floodplain to contribute substantially towards flood risk. However, the fact that (3) corresponds almost exactly with the maximum of $r^*(\boldsymbol{v})$ and (2) is near the secondary maxima of $r^*(\boldsymbol{v})$ suggests that $p(\mathcal{S}|\boldsymbol{v})\phi(\boldsymbol{v})$ is still, in this study, an influential function for calculating risk.

The importance of topography and the influence of different breach failure states have upon flood risk can be considered by referring to a few simulations. Figure 12 shows four flood outlines and their associated damages, $c(s_m, \boldsymbol{v})$, and risks, $r^*(s_m, \boldsymbol{v})$, for single breaches, in which $W = 5.5$ m and $H_s = 2$ m. Despite the same load being imposed on the system, the flood outlines and resultant values of $c(s_m, \boldsymbol{v})$ are very different, and a higher $c(s_m, \boldsymbol{v})$ does not necessarily correspond to a higher $r^*(s_m, \boldsymbol{v})$. This is caused by a number of factors: the system state and its probability of occurrence, the loading on the system, the spatial distribution of the floodplain damages and the floodplain topography. Under more severe loading conditions, multiple component failures account for an increasingly significant proportion of the risk. A comparison of the four very different values of $c(s_m, \boldsymbol{v})$ in figure 12 justifies the use of a computationally demanding inundation model for this case study site.

Dike C breaches: $c(s_m,v)$=~£41 million, $r^*(s_m,v)$=~£50

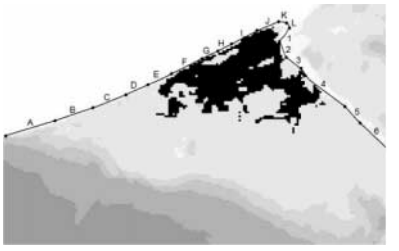

Dike I breaches: $c(s_m,v)$=~£106 million, $r^*(s_m,v)$=~£2000

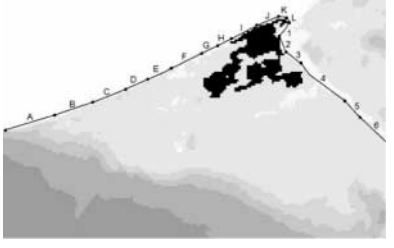

Dike L breaches: $c(s_m,v)$=~£43 million, $r^*(s_m,v)$=~£3500

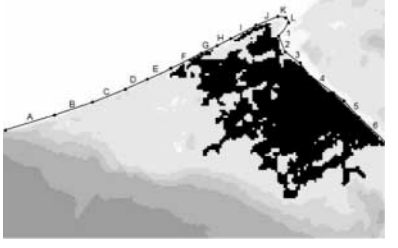

Dike 4 breaches: $c(s_m,v)$=~£79 million, $r^*(s_m,v)$=~£1500

Figure 12. Flood outline (dark shade) and corresponding damage and risk for $H_s=2$ m and $W=5.5$ m for four system failure states.

7. Conclusions

Risk assessment is a well-established technique for measuring the performance of infrastructure systems. A generic methodology for assessing the risk associated with complex infrastructure systems has been developed. The methodology is novel in that the joint space of the loading variables is sampled according to the contribution that a given sub-region of that space makes to *risk* rather than (conventionally) *probability of failure*. This methodology has been applied to a simple beam system and a real coastal dike system.

The use of sampling methods is attractive, as, unlike so-called level II linearization methods, they enable the use of implicit and nonlinear limit state functions. Application of the risk-based sampling methodology on a simple system demonstrates a gain in efficiency of several orders of magnitude relative to a uniform sampling strategy.

In the application to a real coastal dike system in the UK, risk is shown to be a complex function of a number of factors: the system failure state, its probability of occurrence and associated damages and the loading on the system. In this particular case, these are strongly influenced by floodplain topography and the spatial distribution of vulnerable assets in the floodplain. Analysis based only upon conditions at the system design point, or a limited number of breaching failure combinations would not, in the system considered here, have adequately represented important system behaviour. In particular, the location of maximum risk and the design point in the loading space do not coincide.

While the risk assessment methodology has been demonstrated on a coastal dike system, it is more widely applicable than this, but is likely to be most useful where consequences are a nonlinear function of the basic variables and simulation of the system is computationally demanding.

The research described in this paper formed part of the 'RASP: Risk assessment for flood and coastal defence systems for strategic planning' project, funded by joint DEFRA/EA Flood and Coastal Defence R&D programme. The project was managed by Paul Sayers at HR Wallingford and data used in the coastal case study were provided by the Environment Agency, Dr Mohamed Hassan of HR Wallingford and Conwy Borough County Council.

References

Bates, P. D. & De Roo, A. P. J. 2000 A simple raster-based model for flood inundation simulation. *J. Hydrol.* **236**, 54–77. (doi:10.1016/S0022-1694(00)00278-X)

Bates, P. D., Dawson, R. J., Hall, J. W., Horritt, M. S., Nicholls, R. J., Wicks, J. & Hassan, M. 2005 Simplified two-dimensional modelling of coastal flooding for risk assessment and planning. *Coast. Eng.* **52**, 793–810. (doi:10.1016/j.coastaleng.2005.06.001)

Bucher, B. G. 1988 Adaptive sampling—an iterative fast Monte Carlo procedure. *Struct. Safety* **5**, 119–126. (doi:10.1016/0167-4730(88)90020-3)

Casciati, F. & Faravelli, L. 1991 *Fragility analysis of complex structural systems*. Taunton, UK: Research Studies Press.

CIRIA 1996 *The beach management manual, CIRIA R153*. (1996). London, UK: CIRIA.

CUR and TAW 1990 In *Probabilistic design of flood defences* (ed. G. J. H. Vergeer). CUR Report 141 Rotterdam, The Netherlands: Balkema.

Dawson, R. J. & Hall, J. W. 2003 Probabilistic condition characterisation of coastal structures using imprecise information. In *Proc. 28th Int. Conf., Cardiff, UK, 8–12 July 2002*, vol. 2, (ed. J. McKee Smith), pp. 2348–2359. Hackensack, NJ: World Scientific.

Halcrow, HR Wallingford & John Chatterton Associates 2001 *National appraisal of assets of risk from flooding and coastal erosion including the effects of climate change*. London, UK: DEFRA.

Hawkes, P. J., Gouldby, B. P., Tawn, J. A. & Owen, M. W. 2002 The joint probability of waves and water levels in coastal engineering. *J. Hydraul. Res.* **40**, 241–251.

HM Treasury 2001 *Management of risk: a strategic overview*. London, UK: HM Stationery Office.

Horritt, M. S. & Bates, P. D. 2001 Predicting floodplain inundation: raster-based modelling versus the finite-element approach. *Hydrol. Process.* **15**, 825–842. (doi:10.1002/hyp.188)

HR Wallingford 1999 Overtopping of seawalls: design and assessment manual. R&D Technical Report W178. Wallingford, UK: HR Wallingford.

HR Wallingford 2004 Investigation of extreme flood processes & uncertainty. (IMPACT) EC Research Project no. EVG1-CT2001-00037. See www.impact-project.net.

JCSS: Joint Committee on Structural Safety 1981 General principles on reliability for structural design. Int. Assoc. for Bridge and Structural Engineering.

Madrell, R. J., Reeve, D. E. & Heaton, C. R. 1998 Establishing coastal flood risks from single storms and the distribution of the risk of structural failure. In *Proc. Coastlines, Structures and Breakwaters, London, 1998*. London, UK: Thomas Telford.

McKay, D. J. C. 2003 *Information theory, inference, and learning algorithms*. Cambridge, UK: Cambridge University Press.

Melchers, R. E. 1989 Importance sampling in structural systems. *Struct. Safety* **6**, 3–10. (doi:10.1016/0167-4730(89)90003-9)

Melchers, R. E. 1990 Search-based importance sampling. *Struct. Safety* **9**, 117–128. (doi:10.1016/0167-4730(90)90003-8)

Melchers, R. E. 1999 *Structural reliability analysis and prediction*, 2nd edn. New York: Wiley.

Morgan, B. J. 1984 *Elements of simulation*. London, UK: Chapman & Hall.

National Research Council 1992 *Risk assessment in the Federal Government: improving the process*. Washington, DC: National Academy Press.

Penning-Rowsell, E. C., Johnson, C., Tunstall, S. M., Tapsell, S. M., Morris, J., Chatterton, J. B., Coker, A. & Green, C. 2003 *The benefits of flood and coastal defence: techniques and data for 2003*. London, UK: Middlesex University Flood Hazard Research Centre.

Powell, K. A. 1990 Predicting short term response for shingle beaches. Report SR 219, HR Wallingford.

Powell, K. A. 1993 Dissimilar sediments: model tests of replenished beaches using widely graded sediments. Report SR 350. Wallingford, UK: HR Wallingford.

Ripley, B. D. 1987 *Stochastic simulation*. New York: Wiley.

Royal Society 1983 *Risk assessment*. London, UK: The Royal Society.

Royal Society 1992 *Risk: analysis, perception and management*. London, UK: The Royal Society.

Shreider, Y. A. (ed.) 1966. *The Monte Carlo method: the method of statistical trials*. Oxford, UK: Pergamon Press.

Stewart, M. G. & Melchers, R. E. 1997 *Probabilistic risk assessment of engineering systems*. London, UK: Chapman & Hall.

Terzaghi, K., Peck, R. B. & Mesri, G. 1996 *Soil mechanics in engineering practice*, 3rd edn. New York: Wiley.

Thoft-Christensen, P. & Baker, J. M. 1982 *Structural reliability theory and its applications*. Berlin: Springer.

Van der Meer, J. W. 1988 Deterministic and probabilistic design of breakwater armour layers. *J. Waterway Port Coast. Ocean Eng.* **122**, 93–101.

Van Gelder, P. H. J. M. & Vrijling, J. K. 1998 The effect of inherent uncertainty in time and space on the reliability of flood protection. In *Safety and reliability. Proc. ESREL '98 Conf., Trondheim, Norway* (ed. S. Lydersen, G. K. Hansen & H. Sandtorv), pp. 451–456. Rotterdam, The Netherlands: Balkema.

Visser, P. J. 1998 Breach growth in sand defences. Communication on hydraulic and geotechnical engineering, TU Delft Report no. 98-91.

Wahl, T. L. 1998 Prediction of embankment dam breach parameters: a literature review and needs assessment. Dams Safety Office: DSO-98-004. See www.usbr.gov/pmts/hydraulics_lab/twahl/.